Optics Communications 326 (2014) 126–129

Contents lists available at ScienceDirect

Optics Communications

journal homepage: www.elsevier.com/locate/optcom

Direct near-field optical imaging of plasmonic interference fields for high-resolution photolithography

Fu Han Ho *

Graduate Institute of Applied Science and Technology, National Taiwan University of Science and Technology, No. 43, Section 4, Keelung Rd.,Taipei 106, Taiwan, ROC

ARTICLE INFO

Article history:
Received 19 December 2011
Received in revised form
10 April 2014
Accepted 12 April 2014
Available online 26 April 2014

Keywords:
Nano-optics
Near-field optics
Nanophotonics
Plasmonics
Photolithography

ABSTRACT

The plasmonic interference fields on the sub-wavelength gold gratings were directly investigated by using the collection-mode near-field scanning optical microscopy. For proper designs of structural size and periodicity of gratings, we found the plasmonic interference fields generated in the near filed on the gold strip surface. The light source was a visible laser, with a wavelength of 514 nm, illuminating in a normally incident direction to the sample. We demonstrated that the patterns of plasmonic interference fields can reach a narrow linewidth of $\lambda/7$, which is considerably beyond the diffraction limit. The examined widths of the near-field intensities achieved 75–90 nm on the gold strip surface and 110–120 nm on the slit. We also observed that the near-field intensities from both plasmonic interference fields and near-field light of the slits were spatially uniform at the surface, which indicated the capability of near-field intensity redistribution. The numerical simulations by using two-dimensional finite difference time domain (2D-FDTD) method supported the experimental results with excellent consistency. The simulation results also indicated the strong dependences between the plasmon interference fields and polarizations of the incident light. The experimental and simulation results provided the substantial insights for the working mechanism and advanced applications of plasmonic nanopatterns.

1. Introduction

For photolithography, the pattern structures on the photoresists and spatial resolution of the photomask are mainly limited by the optical diffraction, that is, Rayleigh's criterion, and the material properties of photoresists. The light sources with shorter wavelengths, like UV or deep UV light, are consistently used to increase the photomask resolution and reduce the structural size of photoresist patterns. To bypass the diffraction limit, the concept of near-field scanning optical microscopy can be used for optically high-resolution nanofabrication [1–3]. This technology is based on the use of evanescent waves in the optical near field, in which the distance is considerably smaller than the optical wavelength. Technically, the light source with the nanometer size or photomask with subwavelength structures can be used, and placed close to the photoresist surface, which indicates the sub-wavelength distance or direct contact on the surface. The widths of photolithography pattern by using the near-field concept were demonstrated to achieve less than 50 nm [4]. Therefore, the photolithography in the optical near field was developed as a promising method for nanofabrication beyond the diffraction limit.

Recently, several reports proposed the use of metallic nanostructures for the novel photomask in the nanolithography applications, which is called plasmonic lithography, because of their unique optical properties [5–8]. The surface plasmon polariton (SPP) and localized surface plasmon resonance (LSPR) are main factors for the mechanism of those techniques, and their fields are evanescent and localized on the metal/dielectric (or air) interfaces [9,10]. The idea of plasmonic lithography is based on the manipulation of surface plasmon wavelengths at metal/dielectric interfaces, which achieves the nanometer scale (X-ray wavelength) and maintains surface plasmon frequencies in the optical range. Therefore, the higher spatial resolution by using shorter plasmon wavelengths can be obtained and applied for the photolithography and optical imaging. The size, shape, and arrangement of the metallic nanostructures must be considered in an efficient design to manipulate the behaviors of SPP and LSPR. The surface plasmon interference nanolithography (SPIN) technique [11,12], which is one of the plasmonic lithography techniques, was been demonstrated with photoresist patterns and computer simulations to exhibit high-resolution features of approximately 50 nm, created by UV light with metallic masks. The periodic arrangements were

* Tel.: +886 2 27303728; fax: +886 2 27302773.
E-mail address: fuhanho@mail.ntust.edu.tw

http://dx.doi.org/10.1016/j.optcom.2014.04.027
0030-4018/

introduced to produce the resonances and interferences of surface plasmon waves. Several models using various types of nanostructures were frequently proposed and predicted for engineering the plasmon patterns in the nanoscale [13–15], and theoretical simulations also exhibited a noteworthy optical phenomenon for the high-resolution photolithography.

However, the direct experimental measurement of monitoring plasmonic interference fields is limited. Most research consistently demonstrated the linewidth on the photoresist, in which the working mechanism may be mixed by the thresholds of both optical and material effects. In this research, we directly investigated the nano-optical properties of the sub-wavelength gold grating by using a collection-mode near-field scanning optical microscopy (c-mode NSOM). We provided evidence to verify that the patterns of plasmonic interference fields can reach a narrow linewidth that exceeds the diffraction limit. The magnitude and the width of the near-field intensities were simultaneously examined on this periodically sub-wavelength structure. We demonstrated that the width of plasmonic interference fields can be reduced to $\lambda/7$ in the visible wavelength. Compared with the atomic force microscopy (AFM) images, the near-field optical intensities from different origins can be clearly identified. The examined near-field intensities were spatially uniform at the surface which exhibited the function of near-field intensity modulation. In addition, the two-dimensional finite difference time domain (2D FDTD) simulations were studied to provide support to the experimental results.

2. Experiments

Fig. 1(a) shows the experimental setup of c-mode NSOM (Aurora-3, Veeco Instruments Inc.). The NSOM is based on a shear-force-mode AFM configuration with close-loop control system, and a non-optical tuning-fork sensor for feedback control device. The NSOM probe was the pulled fiber tips coated with aluminum with the thickness of 100 nm, and the size of aperture on the fiber tip was 50 nm. A weakly polarized laser light with a wavelength of 514 nm was normally incident from the bottom side of the sample. The near-field scattered lights were collected by aperture of the fiber tip, and detected by using a photo-multiplier tube (PMT). The NSOM fiber tip scanned on the sample surface for imaging the AFM topography and near-field optical intensities simultaneously. The aperture of the probe assumed the function of the photoresist and monitored the near-field optical fields of the surface. The sub-wavelength gold grating was prepared on a gold film with the thickness of 50 nm on a cover glass slide. The gratings were the strip structures with one-dimensionally periodic arrangements, which were fabricated by using a dual-beam focus-ion-beam (FIB) system. The structural sizes were determined by using the scanning electron microscope (SEM), as shown in Fig. 1(b). The widths of gold strips were controlled as 280 ± 15 nm with roughness, and the gap of each slit was 110 ± 10 nm.

Based on theoretical analysis of the surface plasmon waves, the resonant wavelength for normal incident was derived as follow [9]:

$$\lambda_{\mathrm{plasmon}} = \lambda_{\mathrm{structure}} \sqrt{\frac{\varepsilon_{\mathrm{metal}}^{(\omega)} \varepsilon_{\mathrm{surrounding}}}{\varepsilon_{\mathrm{metal}}^{(\omega)} + \varepsilon_{\mathrm{surrounding}}}}$$

for the small corrugation limit, where $\lambda_{\mathrm{structure}}$ is the periodicity of the pattern and ω is the resonance frequency. ε is the dielectric constant for either metal or surrounding materials, depending on the indices. The wave vector of surface plasmons, $k_{sp}=2\pi/\lambda_{\mathrm{plsomon}}$, is considerably larger than that of the free space light at the same frequency by dispersion relations when the real part of $\varepsilon_{\mathrm{metal}}$ approaches $-\varepsilon_{\mathrm{surrounding}}$. According to the conservation of momentum, surface plasmon waves with a wave vector $k_{sp}=2\pi/\lambda_{\mathrm{structure}}$ can be resonantly excited. This formula leads to shorter wavelength of surface plasmon waves with the accurate design of the periodic structures, and indicates the increase of the spatial resolution of surface plasmon waves.

Fig. 2(a) shows the experimental results of the AFM topography and near-field optical intensity images. The AFM topography image indicates the location and size of the gold strips and slits. We found the near-field optical intensities occurred on both the slits and gold strip surface in the NSOM images. The near-field

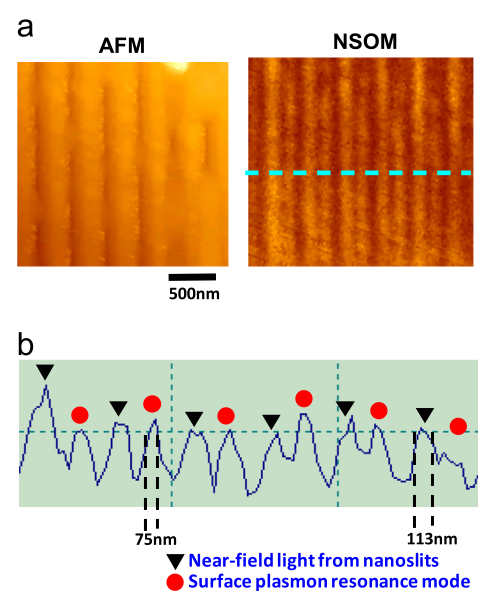

Fig. 2. (a) Experimental results of topographic imaging (left) and near-field optical intensity imaging (right). (b) Cross-sectional profile of near-field optical intensity (corresponding to the dashed line).

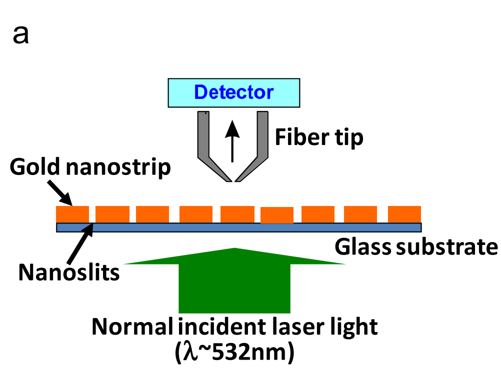

Fig. 1. (a) Experimental setup of c-mode NSOM system. (b) SEM micrograph of the sub-wavelength gold gratings produced using FIB system.